The structures of small gold cluster anions as determined by a combination of ion mobility measurements and density functional calculations

Filipp Furche, Reinhart Ahlrichs, Patrick Weis,[a] Christoph Jacob, Stefan Gilb, Thomas Bierweiler, and Manfred M. Kappes
Institut für Physikalische Chemie, Universität Karlsruhe, Fritz-Haber-Weg 4, 76128 Karlsruhe, Germany

(Received 24 May 2002; accepted 26 July 2002)

A combined experimental and theoretical study of small gold cluster anions is performed. The experimental effort consists of ion mobility measurements that lead to the assignment of the collision cross sections for the different cluster sizes at room temperature. The theoretical study is based on *ab initio* molecular dynamics calculations with the goal to find energetically favorable candidate structures. By comparison of the theoretical results with the measured collision cross sections as well as vertical detachment energies (VDEs) from the literature, we assign structures for the small Au_n^- ions ($n<13$) and locate the transition from planar to three-dimensional structures. While a unique assignment based on the observed VDEs alone is generally not possible, the collision cross sections provide a direct and rather sensitive measure of the cluster structure. In contrast to what was expected from other metal clusters and previous theoretical studies, the structural transition occurs at an unusually large cluster size of twelve atoms. © *2002 American Institute of Physics.* [DOI: 10.1063/1.1507582]

I. INTRODUCTION

The properties of small metal clusters have been in the focus of a large number of experimental and theoretical investigations for more than two decades.[1–5] From the theoretical point of view one might classify these metal clusters according to the difficulties they present for an accurate calculational treatment. In this sense, alkali-metal clusters proved particularly useful in that they were at once comparatively easy to generate experimentally and amenable to computational quantum chemistry. As a consequence, it has proven possible to assign and understand the geometric structures of sodium clusters by comparison of calculated and measured absorbance spectra—for sizes up to more than ten atoms.[6,7] In short, there is a strong tendency to maximize the number of bonds per atom leading to a transition from planar to three-dimensional structures at very small cluster sizes of about six atoms, depending on charge state. Much less is known for transition-metal clusters where electronic structure and chemistry are dominated by the interplay between *s* and *d* electrons. In a sense, the coinage metals (Cu, Ag, Au) with their filled *d* shell can be regarded as a bridge between the ''simple'' *s*-only alkali metal and the more complicated transition metals. As a result they have become the object of numerous experimental[8–17] and theoretical studies.[18–23] Especially silver clusters have been intensely studied.[8,9,11,12,23,24] We have recently shown with ion mobility measurements[25] that, starting at $n=5$, silver cluster cations form compact three-dimensional (3D) structures, in line with theoretical predictions of Bonačić-Koutecký *et al.*[24] In comparison to silver, much less is known about gold clusters, partly because an accurate theoretical treatment requires the inclusion of relativistic effects.[26] Recently Häkkinen and Landman[27] and Grönbeck and Andreoni[28] carried out density functional studies on neutral and anionic gold clusters and predicted minimum structures up to the decamer. Häkkinen and Landman[27] located the planar–3D transition at $n=7$. Experimental inferences related to structure and energetics of isolated gold clusters include collision-induced dissociation studies of singly and multiply charged ions,[15,29,30] photoelectron spectra of gold cluster anions,[11,12,17,31] electronic one-photon dissociation probes of gold clusters (cations and neutrals) complexed to xenon[32] as well infrared multiphoton dissociation spectra of cluster cations with adsorbed sensor molecules.[16,21] Recently we were able to assign the structures of small gold cluster cations ($n<14$) by a combination of ion mobility measurements and density functional theory (DFT) calculations.[33] In short, we found that cationic gold clusters are planar up to $n=7$; starting at Au_8^+ they form three-dimensional structures. For gold cluster anions, the only (indirect) structural data comes from a zero kinetic energy (ZEKE) photoelectron spectroscopy (PES) measurement on Au_6^- (which inferred a planar highly symmetric geometry from resolved vibrational structure[31]).

Here we report on a structural assignment of gold cluster anions by means of gas-phase ion mobility measurements. This method has been proven to be a powerful tool to gain geometric information for molecular ions in the gas phase. It involves the determination of the time it takes for an ion to drift through a gas-filled cell guided by a static electrical field. If we compare two ions of the same mass, the larger molecule will have a longer drift time than the smaller, more compact ion, i.e., it has a larger collision cross section. This cross section allows us to determine the structures of the cluster ions since it can be compared with cross-section predictions from theory (see below). The ion mobility method as such was first developed by Mason and McDaniel.[34] More

[a]Author to whom correspondence should be addressed.

recently, Bowers and co-workers[35,36] combined this method with modern mass spectrometry, and Jarrold and co-workers have applied the technique to a variety of semiconductor and metal cluster ions, especially aluminum, silicon, tin, and lead.[37–40]

II. EXPERIMENTAL SETUP AND METHODOLOGY

The experimental setup used to obtain collision cross sections of cluster ions has been described in detail elsewhere.[41] It comprises a combination of a cluster source, a time-of-flight mass spectrometer, an ion mobility drift cell, and a quadrupole mass filter. The cluster source is a variant of a setup used in Ref. 42 with a rotating disk target, pulsed valve (General Valve Corp.) to provide the cooling gas (helium, backing pressure 5–10 bar), and supersonic expansion through a conical nozzle (1-mm orifice). The vaporization laser (Continuum-ND 61, second harmonic, 532 nm, 30 Hz) is focused collinearly through this nozzle onto the rotating target disk. This target is made by soldering a gold foil (0.1-mm thick, 99.9%, Chempur) onto a 50-mm-diam steel sample holder. To enhance the cluster growth, we use a small (10-mm-long, 10-mm-wide) condensation region prior to the expansion through the nozzle into high vacuum $(10^{-5}-10^{-4}\,\mathrm{mbar})$ of the source chamber.

After vaporization/expansion, the ion packet enters the extraction region of the time-of-flight mass spectrometer. All Au_n^- ions are then accelerated by a pulsed electric field (4.5-kV acceleration voltage) at right angles to the primary beam and transferred into the main chamber (900-mm distance). A particular ion mass is isolated by means of a pulsed mass gate, decelerated to the respective injection energy (typically 100-eV laboratory frame) and injected into the drift cell (110-mm-long, 0.5-mm entrance and exit orifices, filled with 8 mbar helium as buffer gas). The ion packet drifts through the buffer gas in the cell under the influence of a weak electric field (drift voltage 50–300 V). After leaving the cell it passes through the quadrupole mass filter (for rejection of possible fragmentation products) and is detected by means of a channeltron electron multiplier. Typically 1% of ions injected into the drift cell are transmitted.

The transient signal from the detector is fed into an EG&G MCS (micro channel scaler) board (2-μs dwell time). Drift time distributions are acquired as a function of the applied drift voltage, and from the plot of the arrival time (distribution maximum) against drift voltage, we obtain the ion mobility and finally the collision cross section. Typical experimental errors of the collision cross section are in the range of $\pm 2\%$.

III. COMPUTATIONAL METHODS

Potential energy surfaces were scanned for minima by *ab initio* molecular dynamics (AIMD) using a classical treatment of nuclear motion. Typical simulation times ranged between 5 and 10 ps, with 1000 or more individual time steps, at temperatures between 500 and 2000 K. The most prominent minima of the potential energy were optimized subsequently. No symmetry constraints were imposed. All calculations were carried out using the Becke–Perdew86 (BP86)

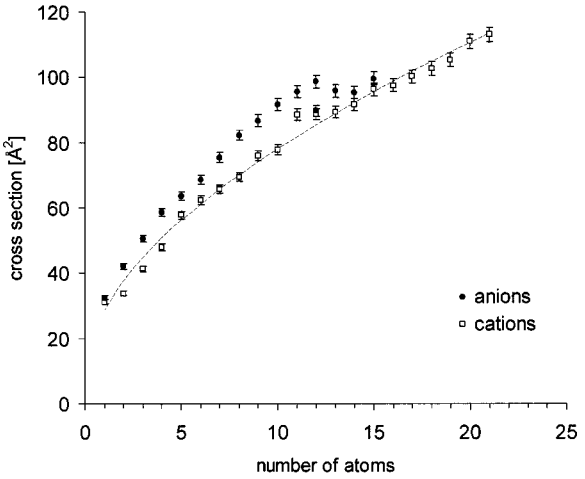

FIG. 1. Cross sections obtained form the ion mobility measurements for positively and negatively charged gold clusters. It is obvious that the small gold cluster anions ($n<13$) have much larger cross sections than the corresponding cations. The dashed line is a fit to the cationic cross sections with the function $\Omega(n)=\frac{4}{3}\pi(n^{1/3}r_{\mathrm{Au}}+r_{\mathrm{He}})^2$. n is the number of atoms, and the parameters r_{Au} and r_{He} are determined to 1.47 and 1.15 Å, respectively. This fit function is used to normalize the calculated and experimental cross sections, i.e., essentially to remove the size dependence of the cross section (cf. Fig. 2).

functional[43] and the resolution of the identity[44,45] (RI) approximation to the Coulomb energy. Grids of m3 quality[46,45] were chosen for the DFT quadrature. Scalar relativistic small-core pseudopotentials with 19 valence electrons[47] were employed. Basis sets were of split-valence plus polarization[45] (SVP) quality for the AIMD simulations; equilibrium structures and energy differences were calculated in the larger $[7s5p3d1f]$ basis described in Ref. 33. For the stationary points found we confirmed that they represent local minima by means of force constant calculations. All calculations were performed using the TURBOMOLE program suite.[48]

In order to actually assign structures one has to compare the experimental cross sections (cf. Fig. 1) with the cross sections of calculated candidate structures. A simple but crude method is to put hard spheres at the atom positions in the (optimized) cluster and calculate its angle-averaged projection area [projection approximation[49] (PA)]. Somewhat more sophisticated is the so-called exact hard-sphere scattering model (EHSS), developed by Shvartsburg and Jarrold.[50] This model incorporates the exact scattering dynamics under the assumption of a purely repulsive potential (hard spheres) centered at the positions of the nuclei. The only adjustable parameter in both the PA and EHSS model is the smallest distance between an atom of the constituent cluster and the buffer gas (helium) atom, i.e., $r_{\mathrm{Au}}+r_{\mathrm{He}}$. These simple models have worked reasonably well for a large number of cationic systems;[36,38–40,49] recently we successfully used them for the structural assignment of gold and silver cluster cations.[25,33]

Due to the electron spill-out the assumption of a fixed atomic radius independent of the cluster size is not a good approximation in anionic systems. Consequently the PA and EHSS method can produce substantial errors ($>5\%$), as has been shown by Jarrold and co-workers in measurements

of silicon[51] and indium[52] cluster anions. They therefore implemented a different approach, the scattering on an electronic density isosurface (SEDI) method: in order to calculate the cross section the candidate structure is not composed of hard spheres, but the contour of the electron density distribution is used instead. This method also contains one adjustable parameter, the threshold electron density above which a volume element in space is considered ''inside'' the molecule, and below which it is ''outside.'' The cross section is then calculated from the overall surface area defined by all the inside volume elements.

The advantage of this method over the hard-sphere approach is that it takes the electron spill-out in anions into account in a natural way (which leads to expansion of the electron density distribution in space). (Our approach is a slight variation of the algorithm of Jarrold and co-workers inasmuch as we use the projected area of the electron cloud instead of an exact elastic scattering on the isosurface.) Since SEDI is (like PA and EHSS) not a parameter-free approach we have to use one gold cluster anion Au_n^- for calibration, i.e., to adjust the threshold electron density so that the experimental and calculated cross sections match. We use the trimeric cluster, Au_3^-, for this purpose, for two different reasons: First, its structure is well known to be linear based on experimental findings[12] and quantum chemical data.[18,19,22] Second, Au_3^- should be large enough that its electron density distribution and helium-cluster–anion interaction potential can be considered typical for the larger anionic gold clusters as well. (The cross sections of the dimer and especially the atomic anion are expected to be significantly more strongly influenced by the extra electron.)

Besides cross sections we have also used another cluster property to benchmark the candidate structures we obtain from theory against the experimental data: Taylor *et al.*[11] and Ho, Erving and Lineberger[12] have measured the vertical detachment energy (VDE), i.e., the energy required to remove the extra electron from the anion by means of photoelectron spectroscopy. This property is easily accessible to calculations, it represents the energy difference between anion and neutral as calculated at the geometry of the anion. We assume that our cluster anion source and injection procedure give rise to the same anions as probed in Refs. 11 and 12.

IV. RESULTS AND DISCUSSION

The experimental cross sections for the gold cluster anions are shown in Fig. 1, together with the results for the gold cations.[33] Included is a fit for cations (dashed line) that assumes near spherical shapes and that describes the larger gold cluster cations ($n>12$) reasonably well. To facilitate the comparison (by essentially removing the size dependence) the cross sections of the anions are divided by this fit function (cf. Fig. 2). It is obvious for all cluster sizes where a comparison can be made that the anions have significantly larger cross sections than the corresponding cations—especially the negatively charged dimers, trimers, and tetramers are effectively more than 20% larger than the corresponding cations. The difference is smaller for the pentamer and hexamer (around 10%), for clusters with 7–10 atoms it

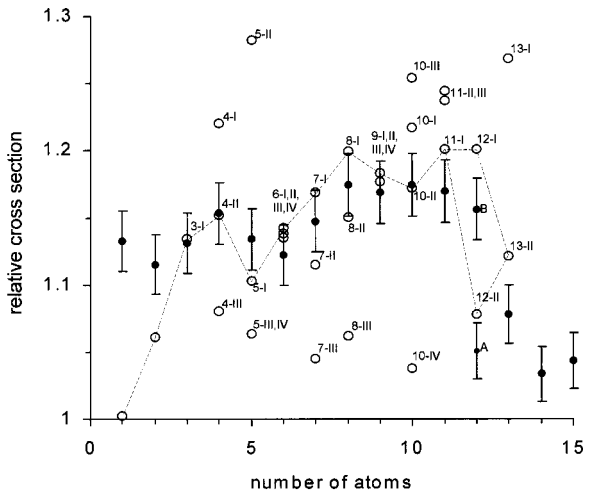

FIG. 2. Relative cross sections of the gold cluster anions obtained by dividing the experimental and calculated cross sections through the fit function $\Omega(n)=\frac{4}{3}\pi(n^{1/3}r_{\mathrm{Au}}+r_{\mathrm{He}})^2$ with $r_{\mathrm{Au}}=1.47$ Å and $r_{\mathrm{He}}=1.15$ Å (cf. Fig. 1). This plot removes the cross-section increase due to the increasing number of atoms per cluster and in this way enhances the effect of the different cluster shapes. The full circles (●) and error bars represent the experimental data. The open circles (○) represent the cross sections of the candidate structures (cf. Table I, Fig. 4). The dashed line connects the ''best'' candidate structures (based on cross section, calculated energy, and vertical detachment energy). In most cases these are lowest in (DFT) energy [labeled with -I (see also Fig. 4 and Table I)]. Exceptions are Au_4^-, Au_{10}^-, and Au_{13}^-, where only candidates that are slightly higher in DFT energy (labeled with -II are in line with experiment.

increases again to 15%–20%, above Au_{10}^- the anion cross sections quickly approach the values for the cationic species–for Au_{15} the difference between cations and anions is only 3.5%. One has to consider two possible reasons for the larger cross sections. First, they may result from larger effective atomic radii for anionic clusters. Second, different structures may pertain for gold cluster cations and anions. The rationale for larger atomic radii comes from the fact that in an anionic cluster the electron cloud is more extended than that in the corresponding neutral cluster, a phenomenon that has been nicknamed ''electron spill-out'' and that has been directly confirmed in mobility measurements of indium clusters.[52] One would expect that this effect quickly decreases with increasing cluster size—the influence of the surplus electron is stronger when there is only a small total number of valence electrons.

In the following we will use the combination of both cross section and VDE data to confirm or rule out the candidate structures obtained from the DFT calculations. PA, EHSS, and SEDI methods differ slightly with regard to cross-section predictions. These differences have no influence on the following structural assignments in which SEDI values are discussed unless otherwise noted. With increasing cluster size the results are as follows.

Au⁻

We obtain in the experiment a cross section for the atomic anion of 32.5 $Å^2$. The calculated value is only 28.8 $Å^2$ [with the electron density threshold calibrated at the trimer (see below)]. Such a comparatively large cross section is

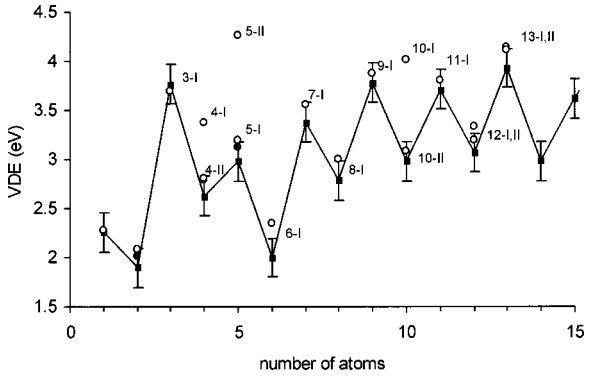

FIG. 3. Experimental and calculated VDE. The full circles (●), squares (■), and error bars represent the experimental data of Ho, Ervin, and Lineberger (Ref. 12) and Taylor *et al.* (Ref. 11), respectively. The open circles (○) represent the VDEs of the candidate structures that are lowest in (DFT) energy [2-I, 3-I,...,13-I (see also Fig. 4 and Table I)] and some of the higher-energy structures.

not unusual for atomic ions and simply reflects the fact that the mobility of Au^- is close to the point charge limit (i.e., dominated by the long-range interaction of the ion charge with the polarizable helium buffer gas and not by the size of the ion as reflecting the short-range repulsive interaction) (cf. Refs. 33 and 34). The electron affinity (calculated as energy difference between Au^- and neutral Au) is 2.28 eV, in excellent agreement with the experimental value of 2.309 eV.[53]

Au_2^-

The calculated DFT bond length is 2.636 Å, in excellent agreement with the relativistic coupled cluster singles and doubles [CCSD(T)] results of Wesendrup, Hunt, and Schwerdtfeger,[22] who obtain a distance of 2.632 Å and also with the experimental value of 2.582±0.007 Å by Ho, Ervin, and Lineberger.[12] With this distance (and the SEDI threshold calibrated at Au_3^-) we calculate a collision cross section of 40.0 $Å^2$; our experimental value is 42.1 $Å^2$. The calculated VDE is 2.09 eV, in reasonable agreement with the experimental data of Taylor *et al.*[11] (1.9 eV) and Ho, Ervin, and Lineberger[12] (2.01±0.01 eV); see Figure 3 and Table I.

Au_3^-

In our calculations we find the lowest-energy structure to be linear (structure 3-I; see Fig. 4). The energetically closest isomer is a triplet state ($^3E'$) with D_{3h} symmetry, it is 1.16 eV higher in energy (structure 3-II). The ground-state Au-Au distance is 2.587 Å. Unfortunately there are no experimental data for this bond distance. Our number is again in excellent agreement with the relativistic CCSD(T) results of Wesendrup, Hunt, and Schwerdtfeger,[22] who obtain a distance of 2.573 Å. It should be noted that the atomization energies ($Au_3^- \rightarrow 2Au + Au^-$) agree surprisingly well: we obtain 4.84 eV, Wesendrup, Hunt, and Schwerdtfeger 4.76 eV.[22] Experimentally known from PES data is the vertical detachment energy, Taylor *et al.* find 3.77±0.2 eV;[11] we calculate 3.69 eV (Fig. 3). The fact that experimental as well as higher-level theoretical results are quite well reproduced by our DFT calculations suggests that DFT is reliable for the larger clusters as well. Our experimental cross section is 50.7 $Å^2$; we adjust the electron density threshold to match this value and obtain $0.0253\,e/Å^3$. This density threshold is used in all cross section calculations for all cluster sizes.

Au_4^-

In the calculations we find three different isomers within an energy range of 0.15 eV. The lowest is a zig-zag chain (4-I; cf. Fig. 4). It has a cross section of 62.0 $Å^2$. A linear form ($D_{\infty h}$ symmetry) is 0.07 eV higher in energy but does not represent a local minimum. Only 0.02 eV above the zig-zag chain is a Y-shaped structure (4-II) with a cross section of 58.5 $Å^2$. This energy difference is clearly smaller than the error inherent in the computational method, which we estimate to be about 0.05–0.1 eV in this size range. 0.14 eV higher is a rhombic structure (4-III) with a cross section of 54.9 $Å^2$. The experimental cross section is 58.6 $Å^2$, which is in almost perfect agreement with the value of the Y-shaped structure 4-II, while we can clearly rule out both the zig-zag chain and the rhombus on the basis of the mobility measurement. This assignment is also in line with the VDEs: the experimental value of Ho, Ervin, and Lineberger[12] is 2.79 ±0.05 eV; Taylor *et al.*[11] obtained a somewhat lower value of 2.63±0.2 eV. The calculated VDEs for structures 4-I, II, and III are 3.37, 2.81, and 2.79 eV, i.e., on the basis of these data we can also rule out structure 4-I, but not distinguish between structures 4-II and 4-III. To summarize, only the Y-shaped structure 4-II is compatible with both the VDE and mobility data.

Au_5^-

The lowest-energy isomer we find is a W-like planar structure, 5-I. It has a calculated cross section of 62.0 $Å^2$. The experimental value is in reasonable agreement, 63.7 $Å^2$. Both Häkinnen and Landman[27] and Grönbeck and Andreoni[28] find the same structure as the global minimum. Its VDE is calculated as 3.2 eV, which is in good agreement with the available experimental data [2.98±0.2 eV (Ref. 11) and 3.12±0.05 eV (Ref. 12)]. A V-shaped chain (5-II) is only 0.13 eV higher in energy. It can be ruled out however, since both its cross section of 72.1 $Å^2$ and the VDE of 4.26 eV do not agree with experiment. Another planar (X-like) structure, which is the most favorable cationic structure,[33] is 0.66 eV higher in energy and does not represent a local minimum. The lowest three-dimensional structure is a square pyramid (5-III); it is 1.02 eV higher in energy than structure 5-I and has a cross section of 59.8 $Å^2$, clearly smaller than the experimental value.

On the other hand, the VDE of this structure is 3.27 eV. Like the VDE of structure 5-I this is reasonably close to the experimental data.[11,12] This also implies that the VDE is not always an unequivocal distinction criterion between different candidate structures (cf. the VDEs of structures 4-II and 4-III). It represents only a useful tool to *rule out* a candidate structure. The (distorted) trigonal bipyramid (structure 5-IV) is even higher in energy (+1.24 eV), and its cross section of 59.8 $Å^2$ is also significantly smaller than the experimental value. On the other hand, the VDE of this isomer calculates to 3.15 eV, again in line with experiment. To summarize,

TABLE I. Calculated and experimental cross sections (in Å^2) relative energies (in eV) and vertical detachment energies (in eV).

	Symmetry	State	Relative E	Ω_{calc}[c]	Ω_{expt}	VDE (calc)	VDE (expt)
1				28.8	32.5		
2	$D_{\infty h}$	$^2\Sigma_g^+$		40.0	42.1	2.09	1.9,[d] 2.01±0.01[e]
3-I	$D_{\infty h}$	$^1\Sigma_g^+$	0	50.7	50.7	3.69	3.77[d]
3-II[a,b]	D_{3h}	$^3E'$	+1.16			2.62	
4-I[a,b]	C_{2h}	^2A_g	0	62.0	58.6	3.37	2.63,[d]
4-II	C_{2v}	$^2A_1$	+0.02	58.5		2.81	2.79±0.05[e]
4-III[a]	D_{2h}	$^2A_{1g}$	+0.14	54.9		2.79	
5-I	C_{2v}	$^1A_1$	0	62.0	63.7	3.2	2.98,[d]
5-II[a,b]	C_{2v}	$^1A_1$	+0.13	72.1		4.26	3.12±0.05[e]
5-III[a]	C_{4v}	$^1A_1$	+1.02	59.8		3.27	
5-IV[a]	C_{2v}	$^1A_1$	+1.25	59.8		3.15	
6-I	D_{3h}	$^2A_1'$	0	69.9	68.6	2.35	2.0[d]
6-II[b]	C_{2v}	$^2A_1$	+0.14	69.6		2.59	
6-III[b]	C_{2h}	^2A_g	+0.23	69.4		3.44	
6-IV[b]	C_{2v}	$^2A_1$	+0.28	69.9		3.86	
6-V[a]	C_s	$^2A'$	+0.61	66.4		3.00	
7-I	C_{2v}	$^1A_1$	0	76.8	75.4	3.55	3.38[d]
7-II[a,b]	C_{2v}	$^1A_1$	+0.50	73.3		3.87	
7-III[a]	C_{3v}	$^1A_1$	+0.67	68.7		3.58	
8-I	D_{4h}	$^2A_{1g}$	0	84.1	82.3	3.0	2.79[d]
8-II[a]	C_{2v}	$^2A_1$	+0.21	80.6		3.13	
8-III[a]	C_{2v}	$^2A_1$	+0.95	74.4		2.74	
9-I	C_{2v}	$^1A_1$	0	87.8	86.7	3.87	3.78[d]
9-II	C_{2v}	$^1A_1$	+0.21	87.6		3.61	
9-III[b]	D_{2h}	$^1A_1$	+0.77	87.3		3.19	
9-IV	C_{4v}	$^1A_1$	+0.39	87.3		3.69	
10-I[b]	C_{2v}	$^2A_1$	0	95.0	91.7	4.02	2.98[d]
10-II	D_{2h}	^2A_g	+0.15	91.5		3.08	
10-III[a]	C_{2h}	^2A_g	+0.31	97.9		3.22	
10-IV[a]	C_s	$^2A_1$	+1.41	81.0		2.88	
11-I	C_s	$^1A_1$	0	98.3	95.7	3.81	3.71[d]
11-II[a]	C_{2v}	$^1A_1$	+0.05	101.2		3.98	
11-III[a]	D_{2h}	^1A_g	+0.17	101.8		3.84	
11-IV[a]	C_s	$^1A'$	+0.22	101.7		3.78	
11-V[b]	C_s	$^1A'$	+0.24	94.3		4.06	
11-VI	C_s	$^1A'$	+0.27	98.9		3.62	
12-I	D_{3h}	$^2A_1'$	0	102.6	89.7	3.34	3.07[d]
12-II	C_{2v}	$^2A_1'$	+0.65	92.6	98.8	3.20	
13-I[a]	C_s	$^1A'$	0	112.8	95.8	4.14	3.93[d]
13-II	C_{2v}	$^1A_1$	+0.24	99.7		4.11	

[a]Structures that can be ruled out on the basis of their cross sections.
[b]Structures that can be ruled out on the basis of their vertical detachment energies.
[c]SEDI values referenced to Au_3^-.
[d]Reference 11.
[e]Reference 12.

based on the cross-section data and on the large energy differences there is no doubt that Au_5^- has a W-like planar structure (5-I), even though the VDE data are compatible with the 3D structures 5-III and 5-IV as well.

Au_6^-

The lowest energy structure we find is highly symmetrical and planar: It is an isosceles triangle (6-I, D_{3h} symmetry). This structure has a cross section of 69.9 Å^2, in good agreement with the experimental value of 68.6 Å^2. It is the same structure that Häkkinen and Landman find[27] and it is also in line with the vibrationally resolved ZEKE PES data of Ganteför, Cox, and Kaldor.[31] We find several other planar isomers, 6-II, 6-III, and 6-IV, within 0.3 eV. Unfortunately their cross sections agree with that of 6-I within 0.5 Å^2. We can, however, clearly rule out three-dimensional structures: The lowest-energy three-dimensional structure 6-V is 0.6 eV higher in energy and its cross section of 66.4 Å^2 does not agree with the experimental value. The VDE of the hexamer is unusually low, 2.0 eV according to the measurement of Taylor *et al.*[11] According to our calculation only isomer 6-I is in reasonable agreement with this value (2.34 eV; see Fig. 3) while the structures 6-II–6-V have VDEs that are significantly larger (2.59, 3.44, 3.86, and 3.00 eV).

Au_7^-

According to our calculations the lowest-energy structure of the heptamer is also planar. It can be looked upon as square with three of its edges bridged by additional gold atoms (7-I). It has a cross section of 76.8 Å^2, which agrees

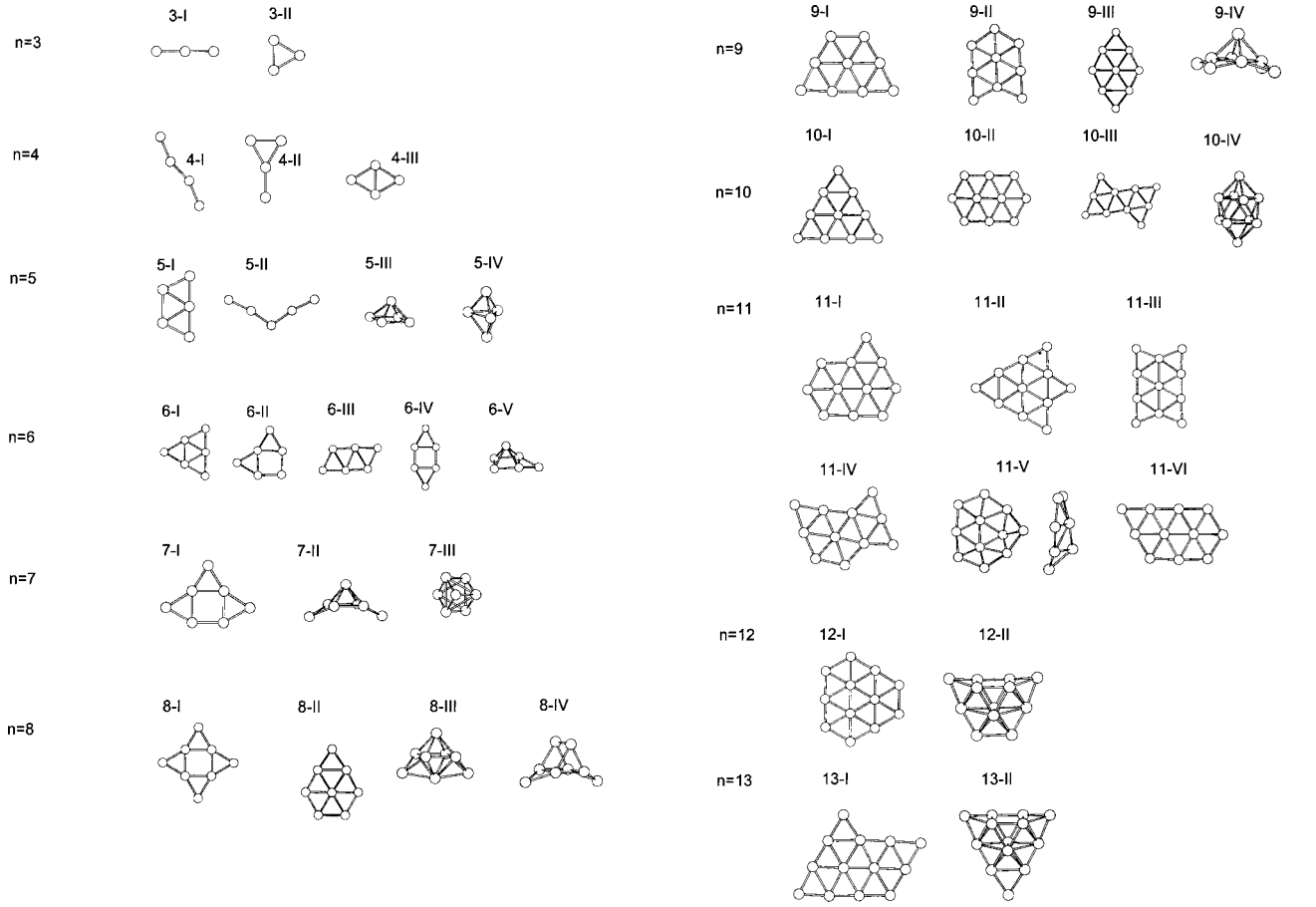

FIG. 4. Candidate structures from full geometry optimizations (within the symmetry indicated in Table I). For respective energies and cross sections see also Table I. The structures in the first row (3-I,4-I,5-I,...) represent the structures that are energetically most favorable at the DFT level.

with the experimental value of 75.4 $Å^2$ within experimental error. The VDE of this structure is 3.55 eV, in good agreement with the experimental value of 3.38 eV.[11] We find only one other isomer within 0.5 eV: It is three-dimensional and consists of a square pyramid with two of its base atoms bridged by additional atoms (7-II). Its cross section of 73.3 $Å^2$ significantly deviates from the experimental value as does its calculated VDE of 3.87 eV. Therefore we can rule out that structure not only for energetical reasons but also on the basis of the mobility and VDE data. The lowest-energy heptamer structure found by Häkkinen and Landman[27] (7-III) is 0.67 eV above structure 7-I and can also be ruled out on the basis of the cross section of 68.7 $Å^2$. Note, however, that the VDE of this structure is 3.58 eV, essentially the same as for the planar structure 7-I and in line with the experimental VDE [3.38 eV (Ref. 11)]. Again, the VDE proves to be an insufficient distinction criteria. We investigated a series of 20 other candidate structures, including the pentagonal bipyramid and the hexagonal ring with one central atom. These structures represent the global minima for Ag_7^+ (Ref. 25) and Au_7^+ (Ref. 33), respectively. For the anion Au_7^- they can be clearly ruled out since both are on the order of 0.85 eV higher in energy.

Au_8^-

For the octamer we find a highly symmetrical (D_{4h}), ''starlike'' planar structure (8-I) to be lowest in energy. It has a collision cross section of 84.1 $Å^2$ in good agreement with the experimental value of 82.3 $Å^2$. Furthermore, its VDE of 3.0 eV agrees reasonably well with the measurement of Taylor *et al.* (2.79 eV).[11] Closest in energy (+0.21 eV) is another planar structure, 8-II, basically a central atom hexagonal ring with one edge bridged. Its cross section of 80.6 $Å^2$ is somewhat lower but also in line with the experimental data. The VDE of this structure is 3.13 eV, which also is in reasonable agreement with experiment (albeit 8-I agrees better). We therefore cannot strictly rule out structure 8-II. We have not found any low-lying three-dimensional structures: The lowest three-dimensional structure we find is a bicapped octahedron (8-III), the favored structure found by Häkkinen and Landmann.[27] According to our calculation it is, however, 0.95 eV above 8-I and has a cross section of 74.4 $Å^2$, 10% below the experimental value. Its VDE is 2.74 eV, not much different from the value of 8-I and the experimental number. ''See also note added in proof''.

Au_9^-

Again we find a planar structure to be lowest in energy, structure 9-I (Fig. 4). This structure is based on a hexagonal ring (cf. 8-II) and has a collision cross section of 87.8 $Å^2$ very close to the experimental value of 86.7 $Å^2$. The VDE is also in good agreement with the experimental data: the calculation predicts 3.87 eV, and the measurement is 3.78 eV.[11]

Depending on the arrangement of the two extra atoms adjacent to the ring one can think of two other isomers, of C_{2v} and D_{2h} symmetry, 9-II and 9-III. On the basis of the mobility measurements we cannot distinguish between them but they are significantly higher in energy, +0.21 and +0.77 eV. Their VDEs are 3.61 and 3.19 eV, respectively, significantly below the experimental value [3.78 eV (Ref. 11)]. In total, we investigated more than 15 different candidate structures and performed extensive molecular dynamics simulations. The lowest three-dimensional structure we find (9-IV) is based on the ''starlike'' structure for the octamer (8-I) with one additional atom centered on top of the inner four-membered ring, which is 0.39 eV above the favored structure 9-I. In structure 9-IV, essentially eight of its atoms are in one plane and accordingly the cross section of 87.3 Å^2 is not much different from the value for the planar isomers 9-I to 9-III.

Au_{10}^-

For the *cationic* gold decamer we have recently found that it has a fairly compact, three-dimensional structure that can be looked upon as a fragment of the gold bulk structure.[33] When looking at the mobility data alone (cf. Fig. 1) it is clear that the *anionic* decamer must have a completely different, much more extended structure: The cross section of Au_{10}^- is 18% larger than the cross section of Au_{10}^+, much more than what is reasonable due to the ''spill-out'' of the extra electron for such a large cluster. This surprising finding is, however, in agreement with the DFT predictions: In our search for the global minimum we find two planar structures (10-I, 10-II) to be lowest in energy and almost degenerate (10-II +0.15 eV). The calculated collision cross sections are 95.0 and 91.5 Å^2; the first is just above the experimental error, the latter is in excellent agreement with the experimental data of 91.7 Å^2. On the basis of the mobility data we therefore cannot clearly distinguish between the two candidate structures. The situation is less ambiguous when considering the VDE: the experimental number is 2.98 eV;[11] structure 10-I has a calculated value of 4.02 eV, 10-II of 3.08 eV. To summarize, structure 10-II is our most likely candidate structure. Again we performed an extensive search for other isomers. The next higher structure we found (10-III, +0.31 eV) can be ruled out on the basis of the mobility (97.9 Å^2) data. Häkkinen and Landman found a three-dimensional structure, 10-IV, to be lowest in energy—according to our calculations, it is, however, 1.41 eV higher in energy and has a cross section of 81.0 Å^2, clearly smaller than the experimental value. The VDE of this structure is 2.88 eV, in reasonable agreement with experiment. ''See also note added in proof''.

Au_{11}^-

The calculation again predicts planar structures to be lowest in energy; the two lowest 11-I and 11-II (+0.05 eV) are almost degenerate. We find three other structures 11-III–11-VI within 0.27 eV of the lowest. They are all based on a hexagonal ring and essentially planar (11-V is somewhat tilted, slightly bowl-like). On the basis of the mobility measurements we can rule out 11-II, 11-III, and 11-IV since they have cross sections of about 101.5 Å^2 (cf. Table I), significantly above the experimental value of 95.7 Å^2. The cross section of structure 11-V (94.3 Å^2) is in best agreement with experiment, but structures 11-I (98.3 Å^2) and 11-VI (98.9 Å^2) also agree reasonably well. The VDE data support structure 11-I. The calculation predicts 3.82 eV for this structure; the experimental value is 3.71 eV.[11] Structure 11-V can be ruled out since its VDE is above 4 eV (cf. Table I).

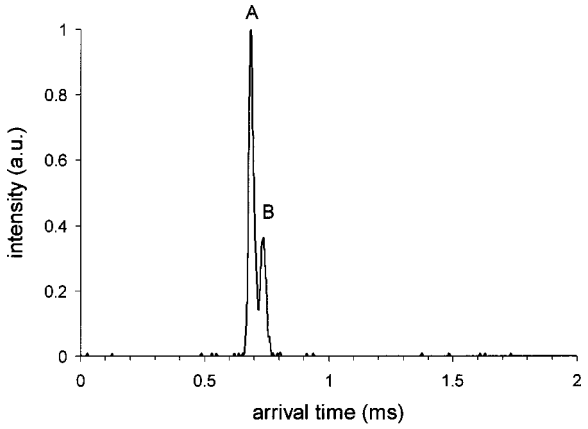

FIG. 5. Typical arrival time distribution of Au_{12}^-. Au_{12}^- is the only cluster size that shows two peaks in the arrival time distribution, i.e., two isomers (*A* and *B*) with largely different cross sections.

Au_{12}^-

The dodecamer is the only cluster size that shows two different peaks in the arrival time distribution, i.e., two isomers with largely different cross sections (see Fig. 5). The first isomer has a cross section of 89.7 Å^2 (isomer *A*), the second of 98.8 Å^2 (isomer *B*). The latter is in line with a planar structure, as can be seen from Fig. 1. The cross section of isomer *A*, on the other hand, is almost identical to that of Au_{12}^+ [which represents a segment of the gold bulk structure, (cf. Ref. 33)] and therefore corresponds to a three-dimensional structure. In the calculation we find a highly symmetric *planar* structure (12-I) to be lowest in energy. The VDE of this structure is 3.34 eV, in good agreement with the experimental value of 3.07 eV.[11] The calculated cross section is 102.6 Å^2, almost 4% larger than the cross section of isomer *B* (98.8 Å^2). This difference is larger than what we found for the smaller cluster sizes and beyond the experimental error limits. A possible explanation is that the structure 12-I is not the structure of isomer *B*. Another possibility is that the structural assignment is correct but that the cross-section calculation with the SEDI method slightly overestimates the cluster size. We tend to this latter possibility because we find that in the SEDI calculations for the cationic gold clusters we need a larger density threshold to fit the experimental data than that for the anionic clusters. Whatever the correct interpretation is, the isomer *B* with the larger cross section must have an open, noncompact structure. Isomer *A* with its cross section of 98.8 Å^2 is in line with a three-dimensional structure, as can be seen from Fig. 1: Its cross section is almost

identical to that of Au_{12}^+, which is three dimensional. We performed an extensive search for a reasonable three-dimensional candidate structure. The most likely candidate we found is structure 12-II with a cross section of 92.6 Å^2, in line with the experimental data for isomer *A*. Its VDE of 3.20 eV agrees with the experimental data; it is, however, 0.65 eV higher in energy than that of structure 12-I, our candidate for isomer *B*. In this size range an exhaustive search for the global minimum becomes overly demanding. Structures 12-I and 12-II should be considered as reasonable candidates for the two isomers, but we cannot rule out other structures.

Au_{13}^-

In the mobility experiment we find one peak with a cross section of 95.8 Å^2. DFT predicts a planar structure based on the same hexagonal tiling that we observed for the smaller clusters [13-I (cf. Fig. 4)]. This structure has a cross section of 112.8 Å^2, 17% larger than experiment, and can be clearly ruled out. Only 0.24 eV higher in energy, we find, however, a three-dimensional candidate structure (13-II) with a cross section of 99.7 Å^2 that is in much better agreement with the mobility measurement. Both structures have essentially the same VDE, 4.14 and 4.11 eV, which agrees with the experimental value of 3.93 eV. Again we cannot rule out other candidate structures for the global minimum—but it is obvious that Au_{13}^- is *not* planar. (Extremely compact 3D structures such as an icosahedron, on the other hand, can also be ruled out—its cross section would be 91.9 Å^2, much smaller than the experimental data.)

Au_{14}^- and Au_{15}^-

As can be seen from Figs. 1 and 2 the experimental cross sections of these clusters approach the values for the gold cluster cations and the quasispherical fit function (dashed line in figure 1), i.e., it is clear that these clusters are three dimensional. On the other hand, exploratory AIMD simulations for Au_{15}^- indicate that planar structures are still favored by the DFT calculations. We conclude that the stability of planar structures is somewhat overestimated by DFT. This behavior is in line with our findings for gold cluster cations[33] and silver cluster cations;[25] in both cases DFT locates the transition to three-dimensional structures 1–2 atoms too high (based on the cross-section measurements we find Au_8^+ to be the first 3D cationic gold cluster).[33]

The obvious question that arises is why the negatively charged gold clusters are planar for this unusually large size range, up to 12 atoms. A possible rationale comes from the relatively small *s*-*d* separation in gold due to the relativistic lowering of the *s* orbitals: this enables a significant *s*-*d* hybridization in small clusters that favors fewer, but more directional covalent bonds, instead of the highly delocalized bond usually found in *s* metals. This is also supported by the Mulliken population analysis: according to this analysis each gold atom in the cluster size range studied has a *d* occupation of roughly 9.75, i.e., 0.25 electrons per atom are promoted form the 5*d* into the 6*s* (and *p*) shell. In this sense, the fact that DFT overestimates the stability of planar structures relative to three-dimensional geometries may be viewed as a consequence of the spuriously small *s*-*d* separation observed in DFT treatments of transition-metal compounds.[54]

V. SUMMARY

The combination of DFT, VDE, and mobility measurements facilitates an unequivocal distinction between two-dimensional and three-dimensional structures for small anionic gold clusters. For sizes up to 11 atoms (except for 9, where we cannot definitely rule out 9-IV), we find that the gold cluster anions are planar. According to the mobility data, three-dimensional structures set in at $n=12$ (Figs. 1 and 2). DFT seems to overestimate the stability of planar structures somewhat; it predicts Au_{13}^- to be planar, while the experimental data shows that it is three dimensional. The comparison of the vertical detachment energy for the different structures with the experimental data, while very useful to *rule out* a possible candidate, has been shown to be not so helpful for the confirmation of a candidate: especially for Au_4^-, Au_5^-, Au_{12}^-, and Au_{13}^-, completely different isomeric forms have essentially the same VDE. It is a surprising and unexpected result that gold cluster anions are planar up to 11 atoms. The transition from 2D to 3D structures occurs much earlier in all other metal clusters investigated so far (see, for example, Refs. 6, 7, and 25). Relativistic effects seem to provide a plausible explanation for this anomalous behavior of gold. Nevertheless, further experimental and theoretical work is necessary to understand the details of the 2D-3D transitions in metal clusters.

Note added in proof. Recently Hakkinen and Landman[55] repeated the calculations for gold cluster anions, Au_n^-, and confirmed our observation of planar structures, especially the geometries 8-I, 9-I, 10-I, 12-I.

ACKNOWLEDGMENTS

This research was supported by the Deutsche Forschungsgemeinschaft and the SFB195 (''Lokalisierung von Elektronen in makroskopischen und mikroskopischen Systemen''), and by the Fonds der Chemischen Industrie.

[1] A. Herrmann, E. Schuhmacher, and L. Wöster, J. Chem. Phys. **68**, 2327 (1978); K. Selby, M. Vollmer, J. Masui, V. Kresin, W. A. de Heer, and W. D. Knight, Z. Phys. D: At., Mol. Clusters **12**, 477 (1989); M. M. Kappes, Chem. Rev. **88**, 359 (1988).
[2] C. R. C. Wang, S. Pollack, and M. M. Kappes, J. Chem. Phys. **94**, 2496 (1991).
[3] V. Bonacic-Koutecký, P. Fantucci, and J. Koutecký, Chem. Rev. **91**, 1035 (1991), and references therein.
[4] T. P. Martin, S. Bjørnholm, J. Borggren, C. Bréchignac, Ph. Cahuzac, K. Hansen, and J. Pedersen, Chem. Phys. Lett. **186**, 53 (1991).
[5] *Metal Clusters*, edited by W. Ekardt (Wiley, Chichester, 1999).
[6] V. Bonacic-Koutecký, J. Pittner, C. Fuchs, P. Fantucci, M. Guest, and J. Koutecký, J. Chem. Phys. **104**, 1427 (1996).
[7] M. Schmidt, C. Ellert, W. Kronmüller, and H. Haberland, Phys. Rev. B **59**, 10 970 (1999).
[8] A. Terasaki, S. Minemoto, M. Iseda, and T. Kondow, Eur. Phys. J. D **9**, 163 (1999).
[9] D. Schooss, S. Gilb, J. Kaller, M. Kappes, F. Furche, A. Kohn, K. May, and R. Ahlrichs, J. Chem. Phys. **113**, 5361 (2000); **113**, 10413 (2000).
[10] C. Pettiette, S. Yang, M. Craycraft, J. Conceicao, R. Laaksonen, O. Cheshnovsky, and R. Smalley, J. Chem. Phys. **88**, 5377 (1988).
[11] K. Taylor, C. Pettiette-Hall, O. Cheshnovsky, and R. Smalley, J. Chem. Phys. **96**, 3319 (1992).
[12] J. Ho, K. Ervin, and W. Lineberger, J. Chem. Phys. **93**, 6987 (1990).

[13] M. Knickelbein and G. Koretsky, J. Phys. Chem. A **102**, 580 (1998).
[14] D. Leopold, J. Ho, and W. Lineberger, J. Chem. Phys. **86**, 1715 (1987).
[15] J. Ziegler, G. Dietrich, S. Krückeberg, K. Lützenkirchen, L. Schweikhard, and C. Walther, Hyperfine Interact. **115**, 171 (1998).
[16] G. Dietrich, S. Krückeberg, K. Lützenkirchen, L. Schweikhard, and C. Walther, J. Chem. Phys. **112**, 752 (2000).
[17] G. Ganteför, H. Handschuh, H. Moeller, Chia-Yen Cha, P. Bechthold, and W. Eberhardt, Surf. Rev. Lett. **3**, 399 (1996).
[18] K. Balasubramanian and M. Z. Liao, Chem. Phys. **127**, 313 (1988).
[19] C. W. Bauschlicher, Jr., S. R. Langhoff, and H. Partridge, J. Chem. Phys. **91**, 2412 (1989); C. W. Bauschlicher, Jr., Chem. Phys. Lett. **156**, 91 (1989).
[20] V. Bonacic-Koutecký, M. Boiron, J. Pittner, P. Fantucci, and J. Koutecký, Eur. Phys. J. D **9**, 183 (1999).
[21] R. Rousseau and D. Marx, J. Chem. Phys. **112**, 761 (2000).
[22] R. Wesendrup, T. Hunt, and P. Schwerdtfeger, J. Chem. Phys. **112**, 9356 (2000).
[23] V. Bonacic-Koutecký, J. Pittner, M. Boiron, and P. Fantucci, J. Chem. Phys. **110**, 3876 (1999).
[24] V. Bonačić-Koutecký, L. Češpiva, P. Fantucci, and J. Koutecký, J. Chem. Phys. **98**, 7981 (1993).
[25] P. Weis, T. Bierweiler, S. Gilb, and M. M. Kappes, Chem. Phys. Lett. **355**, 355 (2002).
[26] P. Pyykkö, Chem. Rev. **88**, 563 (1988).
[27] H. Häkkinen and U. Landman, Phys. Rev. B **62**, R2287 (2000).
[28] H. Grönbeck and W. Andreoni, Chem. Phys. **262**, 1 (2000).
[29] J. Ziegler, G. Dietrich, S. Krueckeberg, K. Lützenkirchen, L. Schweikhard, and C. Walther, Int. J. Mass. Spectrom. **202**, 47 (2000).
[30] V. Spasov, Y. Shi, and K. Ervin, Chem. Phys. **262**, 75 (2000).
[31] G. Ganteför, D. Cox, and A. Kaldor, J. Chem. Phys. **96**, 4102 (1992).
[32] B. Collings, K. Athanassenas, D. Rayner, and P. Hackett, Z. Phys. D: At., Mol. Clusters **26**, 36 (1993).
[33] S. Gilb, P. Weis, F. Furche, R. Ahlrichs, and M. M. Kappes, J. Chem. Phys. **116**, 4094 (2002).
[34] E. Mason and E. McDaniel, *Transport Properties of Ions in Gases* (Wiley, New York, 1988).
[35] P. Kemper and M. Bowers, J. Phys. Chem. **95**, 5134 (1991).
[36] G. v. Helden, N. Gotts, and M. T. Bowers, Nature (London) **363**, 60 (1993).
[37] R. Hudgins, M. Imai, M. Jarrold, and P. Dugourd, J. Chem. Phys. **111**, 7865 (1999).
[38] M. Jarrold and J. Bower, J. Phys. Chem. **97**, 1746 (1993).
[39] A. Shvartsburg and M. Jarrold, Phys. Rev. Lett. **85**, 2530 (2000).
[40] A. Shvartsburg and M. F. Jarrold, Chem. Phys. Lett. **317**, 615 (2000).
[41] P. Weis, S. Gilb, P. Gerhardt, and M. M. Kappes, Int. J. Mass Spec. **216**, 59 (2002)
[42] T. G. Dietz, M. A. Duncan, D. E. Powers, and R. E. Smalley, J. Chem. Phys. **74**, 6511 (1981); P. Milani and W. A. de Heer, Rev. Sci. Instrum. **61**, 1835 (1990); U. Heiz, F. Vanolli, L. Trento, and W.-D. Schneider, *ibid*. **68**, 1986 (1997).
[43] A. D. Becke, Phys. Rev. A **38**, 3098 (1988); J. P. Perdew, Phys. Rev. B **33**, 8822 (1986).
[44] K. Eichkorn, O. Treutler, H. Öhm, M. Häser, and R. Ahlrichs, Chem. Phys. Lett. **242**, 652 (1995).
[45] K. Eichkorn, F. Weigend, O. Treutler, and R. Ahlrichs, Theor. Chem. Acc. **97**, 119 (1997).
[46] O. Treutler and R. Ahlrichs, Chem. Phys. **102**, 346 (1995).
[47] D. Andrae, U. Haeussermann, M. Dolg, H. Stoll, and H. Preuss, Theor. Chim. Acta **77**, 123 (1990); M. Dolg (private communication).
[48] R. Ahlrichs, M. Bär, H. Horn, and C. Kölmel, Chem. Phys. Lett. **162**, 165 (1989); see http://www.turbomole.de for the current version.
[49] See, for example, G. v. Helden, M.-T. Hsu, N. Gotts, and M. T. Bowers, J. Phys. Chem. **97**, 8182 (1993).
[50] A. Shvartsburg and M. F. Jarrold, Chem. Phys. Lett. **261**, 86 (1996).
[51] A. A. Shvartsburg, B. Liu, M. F. Jarrold, and K.-M. Ho, J. Chem. Phys. **112**, 4517 (2000).
[52] J. Lermé, P. Dugourd, R. R. Hudgins, and M. F. Jarrold, Chem. Phys. Lett. **304**, 19 (1999).
[53] H. Hotop and W. C. Lineberger, J. Chem. Phys. **58**, 2379 (1987).
[54] J. P. Perdew and A. Zunger, Phys. Rev. B **23**, 5048 (1981).
[55] H. Hakkinen, M. Moseler, and U. Landman, Phys. Rev. Lett. **89**, 033401 (2002).